

P211 CRS-STACK-BASED SEISMIC REFLECTION IMAGING – A REAL DATA EXAMPLE

Z. HEILMANN, J. MANN, E. DUVENECK and T. HERTWECK
Geophysical Institute, University of Karlsruhe, Hertzstr. 16, 76187 Karlsruhe, Germany

Summary. In recent years, it was demonstrated in many cases that the *Common-Reflection-Surface* (CRS) stack produces reliable stack sections with high resolution and excellent signal-to-noise ratio. As a by-product of the data-driven stacking process, an entire set of physically interpretable stacking parameters, so-called kinematic wavefield attributes, is determined. These CRS attributes may be even more important than the stack section itself because they can be applied in further processing to solve a number of dynamic and kinematic stacking, modeling, and inversion problems.

In this abstract, we present a recent case study demonstrating the basic steps of CRS-stack-based seismic reflection imaging, namely the CRS stack, the determination of a smooth macrovelocity model via CRS-attribute-based tomographic inversion, and, finally, pre- and/or poststack depth migration. As is shown, not only the poststack but also the prestack depth migration result benefits from this approach. Additional CRS-stack-based processing steps that could also be applied are, e. g., residual static corrections using CRS stacking operators, limited-aperture migration based on the estimated projected Fresnel zone, determination of the geometrical spreading factor, and amplitude-variation-with-offset analysis in the time domain using approximate common-reflection-point trajectories calculated from CRS attributes.

Introduction. The seismic data used for this case study was acquired in the close vicinity of Karlsruhe, Germany by *Deutsche Montan Technologie (DMT) GmbH* along two almost parallel lines having a separation of ≈ 2.5 km and a length of ≈ 12 km each. The acquisition was performed for *HotRock EWK Offenbach/Pfalz GmbH* with the intention to obtain a structural image of the subsurface relevant for a projected geothermal power plant. The latter will be based on two boreholes, reaching a depth of ≈ 2.5 km, where a strongly fractured horizon of hot-water-saturated lacustrine limestone is located. As the achievable production rate depends mainly on the degree of fracturing of the target horizon and the number of faults reached by the boreholes, a detailed knowledge of the subsurface structure is essential.

After preprocessing was carried out, DMT applied a standard imaging sequence, consisting of normal-moveout (NMO) correction/dip-moveout (DMO) correction/stack, finite-differences (FD) time migration, and a time-to-depth conversion using macrovelocity models based on stacking velocity sections.

As an alternative to this, we applied a CRS-stack-based seismic imaging workflow (Hertweck et al., 2003; Mann et al., 2003) in the framework of an ongoing research cooperation with DMT and HotRock, with the purpose to enhance and extend the results obtained so far. Additional steps such as residual static corrections using CRS stacking operators (Koglin and Ewig, 2003), true-amplitude migration, and amplitude-variation-with-offset (AVO) analysis may follow in the near future.

CRS stack. Starting point for the applied CRS-stack-based seismic imaging workflow (Figure 1) was the preprocessed multicoverage seismic reflection data. The preprocessing had been performed in different steps of filtering, amplitude correction, muting, deconvolution, field static correction, and residual static correction. Within the course of this project, the CRS stack method (see, e. g., Jäger et al., 2001; Mann, 2002) was complemented by an algorithm smoothing the obtained CRS attributes in an event-consistent way. Afterwards, the smoothed attributes are used for a final optimization and stacking iteration, resulting in a

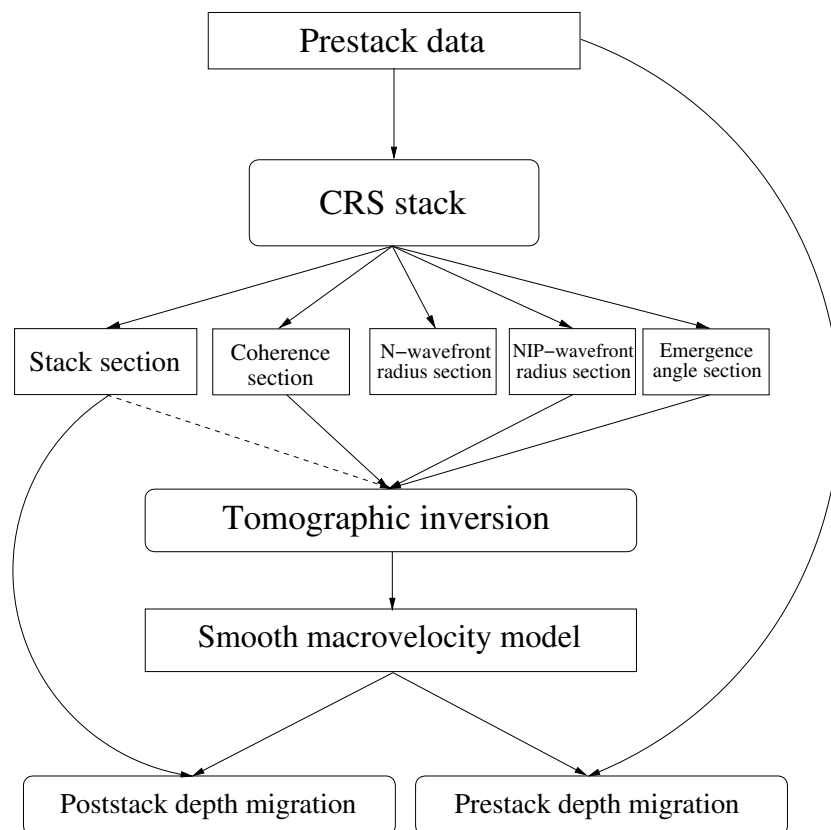


Figure 1: The CRS-stack-based seismic imaging workflow.

significant enhancement of event continuity. The final stack is restricted to the projected first Fresnel zone calculated from the obtained CRS attributes. As depicted in Figure 1, the 2D zero-offset (ZO) CRS stack provides in addition to the stack section a coherence section and three sections of kinematic wavefield attributes. The coherence indicates the fit between the determined CRS stacking operator and the reflection event in the prestack data. The three kinematic wavefield attributes are:

- the curvature of the normal (N) wavefront which would be observed at the emergence point of the ZO ray due to an exploding reflector element at the normal-incidence-point (NIP) of the ZO ray at the reflector.
- the radius of the NIP wavefront as observed at the emergence point of the ZO ray, whereas the NIP wave is defined by focusing at that point of the reflector, where the ZO ray is reflected, i. e., at the NIP.
- the emergence angle of the ZO ray, measured with respect to the top-surface normal.

Tomographic inversion. In order to obtain a depth image from the time-domain pre- and/or poststack data, a kinematically correct macrovelocity model needs to be constructed. Such a model can be obtained directly from the CRS stack results by means of a tomographic inversion method based on the kinematic wavefront attributes associated with the NIP wave (Duvencq, 2004). As depicted in Figure 1, these attributes are the radius of curvature of the NIP wavefront and the emergence angle of the ZO ray. For the description of the smooth macrovelocity model two-dimensional B-splines are used.

In this case study, about 1000 ZO samples together with their respective attribute values were picked for each profile to achieve an appropriate resolution and reliability. To reduce the effort involved in manual picking, the existing software was extended by a module performing automatic picking based on the coherence associated with the ZO samples. The picked data was checked using several criteria, in order to discriminate outliers and attributes related to multiples, before the tomographic inversion process was applied. All in all, the velocity models of the two profiles are very similar. However, considering the small distance between the two seismic lines, the minor differences between the two models reveal a strong lateral inhomogeneity of the investigated subsurface.

Prestack depth migration. Based on the macrovelocity models obtained in the previous step, we applied a Kirchhoff depth migration to the prestack data of both profiles. The necessary kinematic Green's function tables (GFTs) were calculated by means of an eikonal solver. The resulting depth-migrated prestack data was firstly muted to avoid excessive pulse stretch for shallow reflectors and then stacked in offset direction. For the sake of brevity only the depth migrated result of one profile (Figure 3) and some of the respective common-image-gathers (CIGs) (Figure 2) are displayed in this abstract. For both profiles, a multitude of faults and fractures are visible, which are clearly imaged even at larger depths. Compared to the standard processing the CRS-stack-based imaging results offer a higher resolution, especially in the target area. The depth location of the reflectors was assessed to be more reliable by the interpreters.

Poststack depth migration. As a complementary or alternative step of the CRS-stack-based imaging workflow, a poststack depth migration for both profiles was performed. Due to the fact that, unlike as for prestack migration, only the ZO section is migrated to depth, the computational costs of poststack migration are much lower. In addition, poststack depth migration can be advantageous in cases where the determination of a sufficiently accurate macrovelocity model is difficult and/or the signal-to-noise ratio is poor. However, in the case discussed here, where the data quality is very high and the obtained macrovelocity models are reliable, poststack depth migration cannot fully compete against prestack depth migration in view of resolution and image quality, as can be seen in Figure 4. In particular, the faults and fractures are not as well resolved as by the prestack depth migration and the shallow area down to 750 m depth is slightly worse imaged. Nevertheless, there are also regions, especially at greater depths, where some details are better resolved than by the prestack depth migration. Thus, the poststack depth-migrated results can provide complementary information in crucial questions of geological interpretation even in this case.

Conclusions. The great potential of a seismic imaging approach, based on kinematic wavefield attributes obtained by the CRS stack, was demonstrated in a commercial exploration project. Due to the fact that a standard processing sequence was carried out in parallel, the reliability and high quality of the results of the applied CRS-stack-based seismic imaging workflow could be proven. With the obtained results, a very good basis for the geological interpretation and a hopefully successful drilling is available. The target area and the existing faults and fractures were imaged clearly and the high grade of tectonic displacement necessary to ensure a sufficiently large production rate was verified.

Acknowledgments. This work was kindly supported by *HotRock EWK Offenbach/Pfalz GmbH*, Karlsruhe, Germany, the *Federal Ministry for the Environment, Nature Conservation and Nuclear Safety* of Germany, and the sponsors of the *Wave Inversion Technology (WIT) Consortium*, Karlsruhe, Germany. We also like to thank *Deutsche Montan Technologie (DMT) GmbH*, Essen, Germany, for good collaboration during the entire project.

References

- Duveneck, E. (2004). Velocity model estimation with data-derived wavefront attributes. *Geophysics*, 69(1). In print.
- Hertweck, T., Jäger, C., Mann, J., and Duveneck, E. (2003). An integrated data-driven approach to seismic reflection imaging. In *Extended Abstracts, 65th Annual Internat. Mtg., Eur. Assn. Geosci. Eng.*, Session: P004.
- Jäger, R., Mann, J., Höcht, G., and Hubral, P. (2001). Common-reflection-surface stack: Image and attributes. *Geophysics*, 66:97–109.
- Koglin, I. and Ewig, E. (2003). Residual static correction by means of CRS attributes. In *Expanded Abstracts, 73rd Annual Internat. Mtg., Soc. Expl. Geophys.*, pages 1889–1892.
- Mann, J. (2002). *Extensions and applications of the Common-Reflection-Surface stack method*. Logos Verlag, Berlin.
- Mann, J., Duveneck, E., Hertweck, T., and Jäger, C. (2003). A seismic reflection imaging workflow based on the Common-Reflection-Surface stack. *Journal of Seismic Exploration*, 12:283–295.

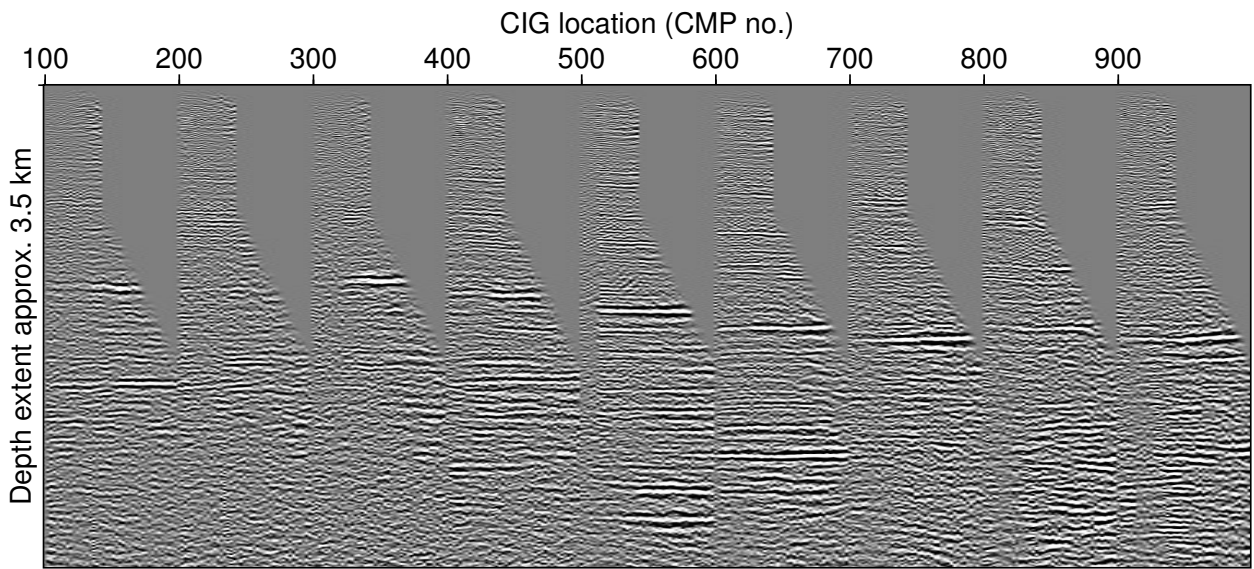


Figure 2: Common image gathers, Profile A.

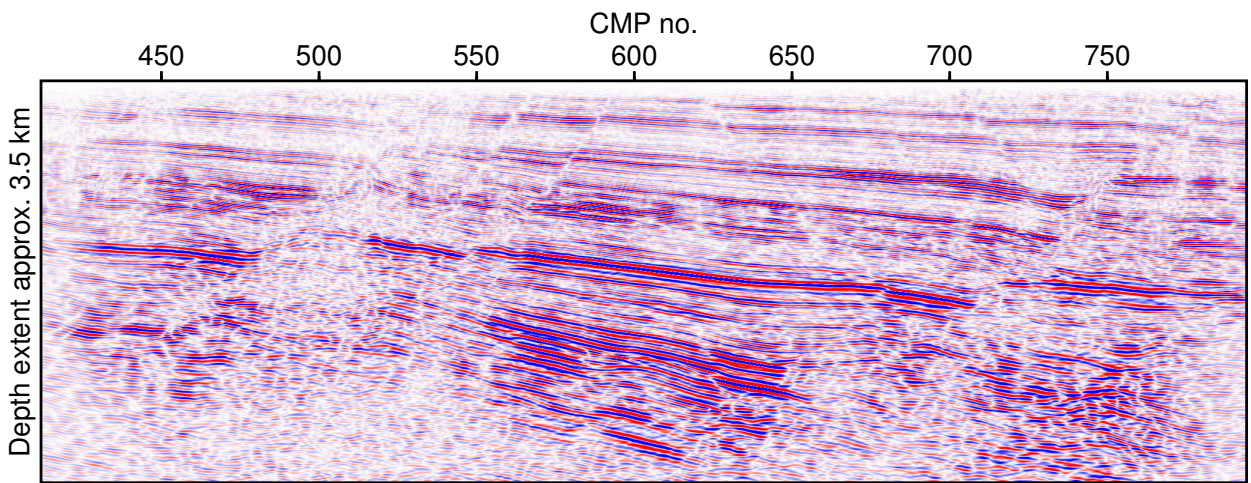


Figure 3: Prestack depth migration result, Profile A.

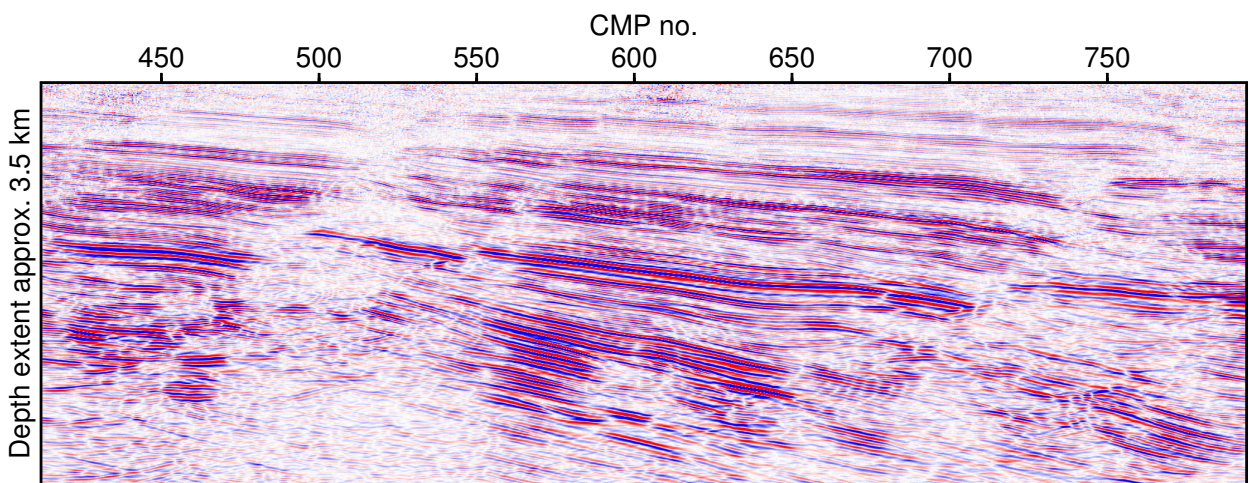


Figure 4: Poststack depth migration result, Profile A.